

CR 73463

AVAILABLE TO THE PUBLIC

N70 32469

~~N70 32469~~

CROSS SECTIONS FOR IONIZATION IN COLLISIONS BETWEEN EXCITED NITROGEN MOLECULES AND CARBON MONOXIDE AND NITROGEN GROUND-STATE MOLECULES

By

Nyle G. Utterback and Bert Van Zyl

JUNE 1970

Distribution of this report is provided in the interest of information exchange.
Responsibility for the contents resides in the author or organization that prepared it.

Prepared under
Contract No. NAS2-5680

by

AC ELECTRONICS-DEFENSE RESEARCH LABORATORIES
General Motors Corporation
(AC-DRL Report No. TR70-55)
Santa Barbara, California

for

AMES RESEARCH CENTER
NATIONAL AERONAUTICS and SPACE ADMINISTRATION

CASE FILE
COPY

~~For U. S. Government Internal Use Only~~

**CROSS SECTIONS FOR IONIZATION IN COLLISIONS BETWEEN
EXCITED NITROGEN MOLECULES AND CARBON MONOXIDE
AND NITROGEN GROUND-STATE MOLECULES**

By

Nyle G. Utterback and Bert Van Zyl

JUNE 1970

Distribution of this report is provided in the interest of information exchange.
Responsibility for the contents resides in the author or organization that prepared it.

Prepared under

Contract No. NAS2-5680

by

AC ELECTRONICS-DEFENSE RESEARCH LABORATORIES

General Motors Corporation

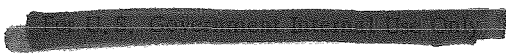
(AC-DRL Report No. TR70-55)

Santa Barbara, California

for

AMES RESEARCH CENTER

NATIONAL AERONAUTICS and SPACE ADMINISTRATION





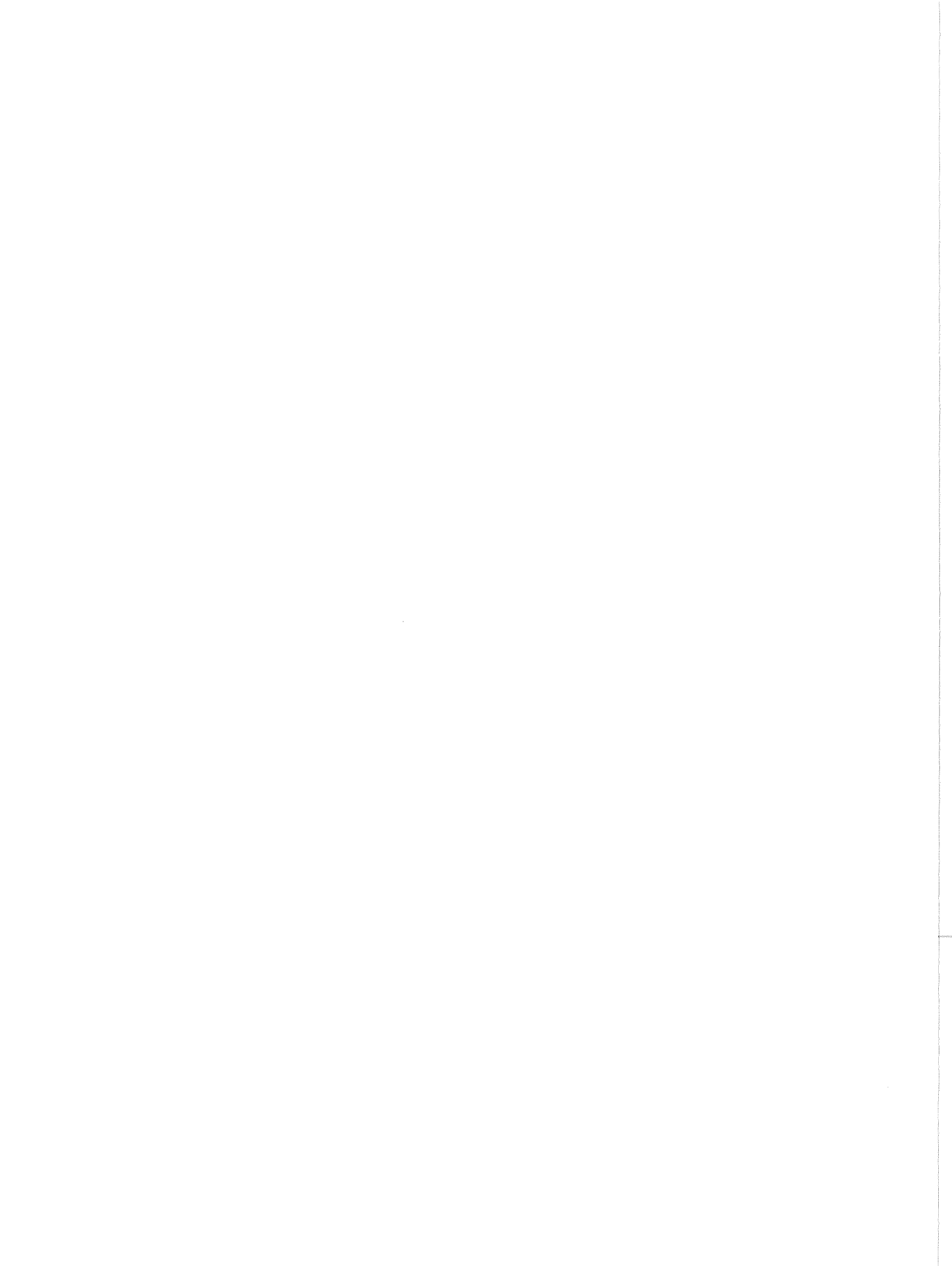
CROSS SECTIONS FOR IONIZATION IN COLLISIONS BETWEEN
EXCITED NITROGEN MOLECULES AND CARBON MONOXIDE
AND NITROGEN GROUND-STATE MOLECULES

by

Nyle G. Utterback and Bert Van Zyl

SUMMARY

A molecular beam containing N_2 molecules in the $A^3\Sigma_u^+$ state has been used to bombard target molecules of ground-state CO and N_2 . The total ionization cross sections have been determined for these collisions at kinetic energies from a few eV above the energy threshold to 100 eV above threshold in the center-of-mass coordinate system. Because no totally unambiguous method has been found to determine the amounts of excited-state and ground-state molecules in the beam, the directly measured cross sections constitute absolute lower limits. However, by subjecting the measured cross section values (including previously studied targets of NO, O_2 , Ar and Au surfaces) to a series of parametric consistency checks, it has been found possible to infer the amounts of excited-state and ground-state molecules in the beam, and therefrom to obtain the actual excited-state cross sections. A comparison of all these cross section values with those obtained using a ground-state N_2 beam indicates that internal electronic energy is more than equivalent to an equal amount of kinetic energy in producing ionization. However, selection rules appear to control the individual ionizing processes which occur. This has been dramatically demonstrated by mass spectrometric studies comparing the processes $N_2 + CO \rightarrow NO^+ + CN^-$ and $N_2 + O_2 \rightarrow NO^+ + NO^{(-)}$ with the N_2 molecules electronically unexcited and excited.



CONTENTS

<u>Section</u>	<u>Page</u>
INTRODUCTION	1
EXPERIMENTAL METHOD	4
Molecular N ₂ Beam	4
Target Chamber	7
Ion Collection and Current Measurement	9
Consistency Checks and Systematic Corrections	10
DIRECTLY MEASURED RESULTS AND RELIABILITY	13
BEAM EXCITATION PARAMETER INFERRAL	23
Excitation Parameters	23
Inferred Excited-State Cross Sections	28
MASS SPECTROMETER MEASUREMENTS	32
DISCUSSION	35
REFERENCES	39

ILLUSTRATIONS

<u>Figure</u>		<u>Page</u>
1	Block Diagram of Apparatus	5
2	Target Configurations	8
3	Composite Total Ionization Cross Section for $N_2^* + CO$. Electron Energy 22 eV	15
4	Composite Total Ionization Cross Section for $N_2^* + CO$. Electron Energy 19 eV	16
5	Composite Total Ionization Cross Section for $N_2^* + CO$. Electron Energy 17.5 eV	17
6	Total Ionization Cross Section for $N_2 + CO$. Ground-State	18
7	Composite Total Ionization Cross Section for $N_2^* + N_2$. Electron Energy 22 eV	19
8	Composite Total Ionization Cross Section for $N_2^* + N_2$. Electron Energy 19 eV	20
9	Composite Total Ionization Cross Section for $N_2^* + N_2$. Electron Energy 17.5 eV	21
10	Total Ionization Cross Section for $N_2 + N_2$. Ground-State	22
11	Inferred Total Ionization Cross Section for $N_2^* + CO$. Excited-State	29
12	Inferred Total Ionization Cross Section for $N_2^* + N_2$. Excited-State	30

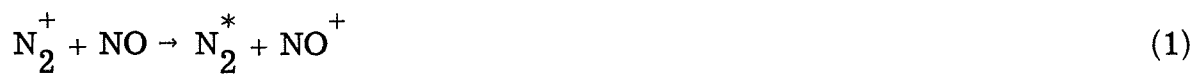
INTRODUCTION

The process of ionization has important consequences in many areas pertinent to hypersonic flight and atmospheric entry, with their attendant extreme high temperature. Measurements of bulk ionization rates are difficult in many regimes of chemical species, pressure, and temperature. At best, the results tend to be gross and to yield little information on detailed ionizing processes. It is thus of interest to develop a model for bulk ionization, from which bulk ionization rates can be calculated. Recently Hansen⁽¹⁾ formally proposed such a model, recognizing that ionization processes between excited collision partners would be an extremely important part of it. His model directly employs kinetic theory in terms of cross sections for ionization, and the reaction rate is determined by straightforward integration over all ionizing collisions. The important feature is that collisions between internally excited collision partners are not ignored, as they were previously. The major difficulty encountered in validating this model has been the lack of information regarding the ionization cross sections. Although a few cross section values for neutral-neutral ionization between ground-state collision partners were available, none had been measured for collisions between excited partners. The present research was initiated to measure a few representative cross sections in this category.

Recently it was found⁽²⁾ possible to produce a fast neutral beam of N_2 molecules in the $A^3\Sigma_u^+$ state (6.3 eV). Since N_2 is a species of some practical importance, and since the A-state has a sufficiently high internal energy to produce observable effects, it was decided to employ $N_2(A)$ as the beam species. For targets, Ar atoms and O_2 , NO, CO and N_2 molecules were picked as representative and tractable. The present report concerns largely the CO and N_2 targets; the others were studied under the preceding contract, NAS2-4924.

The apparatus for producing a nitrogen molecular beam has been described in detail.⁽³⁾ It utilizes production of nitrogen molecular ions by electron bombardment, electrostatic acceleration of the ions into a beam having the desired energy and trajectory, and their neutralization by charge transfer in a suitable gas. Nitrogen has usually been selected as the neutralizing gas because the resonant character of the interaction leads to production of fast ground-state neutrals with a large cross section at low energy. Hydrogen has also been employed, although it is not quite resonant and thus has a smaller charge-transfer cross section at the lowest energies. However, hydrogen has the advantage that the kinetic energy available for excitation (center-of-mass energy) in $N_2^+ + H_2$ collisions is only 1/15 the beam energy, thus putting a limit on the internal excitation which might be present in the N_2 molecular beam.

For the excited beam employed here, nitric oxide was used as the neutralizing gas (bar indicates the fast particle), i. e.,



The charge transfer cross section for these reactants has been measured to be about one-fourth that for N_2^+ in N_2 (i. e., about $9A^2$ at 30 eV). Most significant is the observation that it appears to increase with decreasing energy to below 20 eV, suggesting that a resonant or near-resonant process occurs. A plausible explanation can be found in the energy balance of reaction (1). The N_2^+ has an ionization energy of 15.58 eV and the NO^+ , 9.27 eV, a difference of 6.31 eV. This is very close to the energy of the metastable $A^3\Sigma_u^+$ state of N_2 . Reaction (1) is essentially resonant if this is the excited state populated during the charge transfer. Capture into other excited states of the nitrogen molecule (except for other low-lying vibrational levels of the $A^3\Sigma$ state) would be significantly nonresonant. Furthermore, if other nearby electronic states were to be populated during the collision, some of these (such as the important $B^3\Pi$ state) would decay to the $A^3\Sigma$ level. Transitions from the N_2^+ to the $A^3\Sigma$ state

of N_2 are compatible with the application of the Frank-Condon principle, and the spin-conservation rule is not violated. Unfortunately, the process $N_2^+ + NO \rightarrow N_2(X) + NO^+(a)$ competes with reaction (1). (It was recently found that the accepted energy level for the $NO^+(a)$ state was incorrect, and the new value of 15.5 eV makes this reaction essentially resonant.) This has the effect of introducing a ground-state N_2 component into the beam, and necessitates determining the percentages of excited-state and ground-state molecules in the beam in order to obtain unambiguous excited-state cross sections.

The total ionization cross sections for $N_2^* + CO$ and $N_2^* + N_2$ were measured in the same manner described previously^(4, 5) for $N_2 + N_2$ and $N_2 + O_2$ collisions. The fast, excited molecular beam traversed a low-pressure gas target (10^{-4} torr) between the guarded plates of a parallel-plate ionization chamber. Negative charges arising from ionizing collisions were driven to the collector plate by the electrostatic field between the plates. Particular care was taken to exclude stray secondary electrons ejected by scattered beam molecules. Knowledge of the target number density, collector length, current of negative charges, and neutral beam intensity allowed a determination of the ionization cross section (more precisely, the total cross section for production of negative charges in the collisions). The target number density was determined from the target gas pressure. The neutral beam intensity was inferred from the current of slow ions produced in the charge transfer cell, since each slow ion corresponded to a fast neutral molecule. As pointed out above, because both excited and ground-state molecules were present in the beam, the directly measured cross sections were a composite of excited and ground-state cross sections. Knowledge of the amounts of excited and ground-state molecules in the beam, as well as the ground-state cross sections were needed in order to unfold the actual excited-state cross sections.

The present report also includes mass spectrometer measurements on the products from the ionizing collisions of $N_2 + CO$ and $N_2 + O_2$, with particular regard to the effects of excitation in the N_2 on the individual charged products produced.

EXPERIMENTAL METHOD

Molecular N_2 Beam

The molecular N_2 beam apparatus has been discussed in detail elsewhere.⁽³⁾ A short summary will be given here.

Figure 1 shows a block diagram of the beam-producing apparatus. An N_2^+ ion beam was produced by the ion source and lens system. The ion source was operated as an electron impact source. The electron energy was normally 22 eV, but could be varied from 16 to 25 eV. The N_2 pressure was about 40 microns Hg. The lens system determined the final ion beam energy and focused the ion beam through the apertures behind it. A fraction (<15%) of the ion beam entering the neutralization chamber was neutralized by charge transfer with N_2 or H_2 gas (or NO for the excited beam). The mixed ion and molecular beam passed between deflecting plates where the remaining ions were removed.

The molecular N_2 beam intensity was determined by measuring three currents as follows. The ion collector current was i_1 and corresponded to those ions which had not undergone charge transfer or strong scattering. The current i_2 arose from the charge-transfer cup which was held at a potential positive enough to repel the slow ions arising from charge transfer, but not positive enough to repel scattered ions; i_2 therefore corresponded to ions strongly scattered which had not undergone charge transfer. The ions arising from charge transfer were driven by the positive cup to the grid and were collected

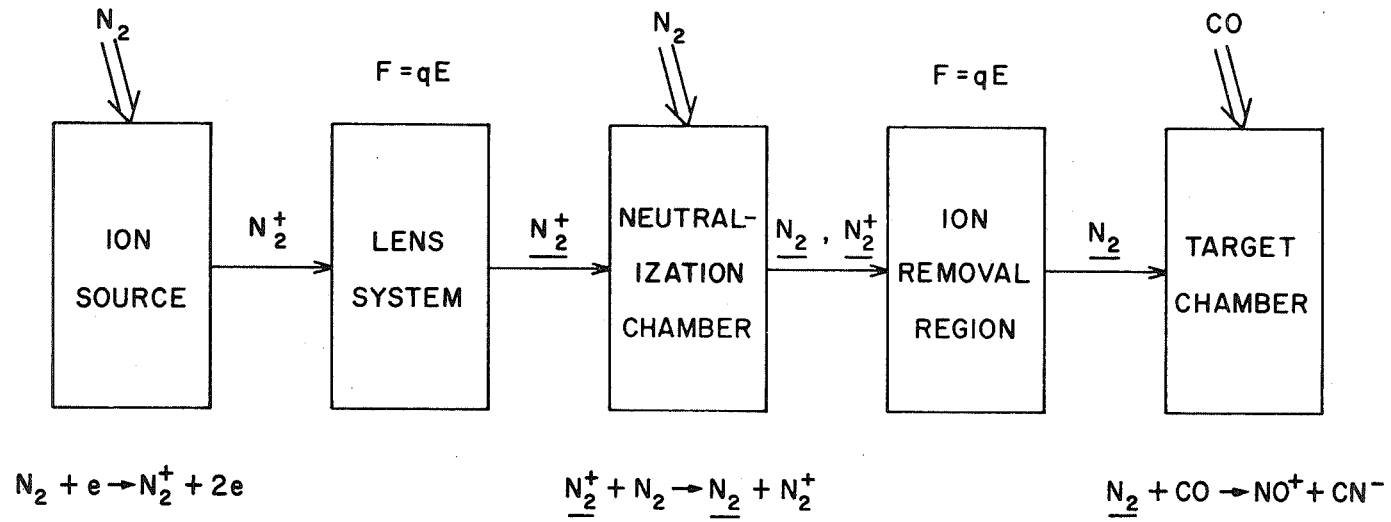


Figure 1 Block Diagram of Apparatus

as i_3 . Now $i_1 + i_2 + i_3$ was the total ion current entering the neutralization chamber. Thus β , the fraction of all entering ions which underwent charge transfer, was given by

$$\beta = \frac{i_3}{i_1 + i_2 + i_3} \quad (2)$$

If I represents the unscattered ion beam in the event charge transfer had not occurred, the current i_1 was given by

$$i_1 = I - \beta I \quad ,$$

or

$$I = \frac{i_1}{1 - \beta} \quad (3)$$

It follows that the molecular beam intensity in molecules per second, B , was

$$B = \beta I = \frac{\beta i_1}{1 - \beta} = \frac{i_3}{1 + i_2/i_1} \quad (4)$$

where the currents are in ions per second.

It is seen that if no scattering were present ($i_2 = 0$), the molecular beam intensity would have been equal to i_3 , the slow ion current. A more detailed discussion of the assumptions implicit in Eq. (4) has been given previously. (3) It was also shown in that reference that the absolute intensity for ground-state beams could be determined to within 20% by the use of this method. Beam intensities of the order of 10^8 to 10^{10} molecules per second were used in this work.

The molecular N_2 beam energy and energy spread were obtained by first measuring the energy and energy spread of the N_2^+ ions entering the neutralization chamber. In order to determine the energy spread and average energy of these N_2^+ ions, the neutralization chamber was used as a Faraday cage. With

no neutralizing gas present, the grid and cup were connected and formed the collector for the Faraday cage. High positive potentials were placed on both the repeller and ion collector in order to electrically close the exit aperture of the cup. The electrode at the entrance aperture of the cup was maintained approximately two volts negative with respect to the equipotential region in front. This focused entering ions away from the aperture edges and thus minimized edge effects caused by changing the Faraday-cage collector potential. A plot of the Faraday-cage collector current as a function of its potential indicated an energy spread at half-maximum of 0.4 eV. The average energy was 1.6 eV less than the ion source-to-neutralization region potential difference. This discrepancy might have been a small ion-source offset caused by the extraction field, or a contact potential difference between the ion source and neutralization region. Molecular beam energies in this work were determined under the assumption that negligible momentum was transferred during charge transfer, and therefore that the neutral beam energy was the same as the ion beam energy. A correction of 1.6 eV was made to the beam energy as discussed above.

Target Chamber

Configuration A in Figure 2 shows the electrode arrangement in the target chamber. The molecular N_2 beam was directed between the grid and the collector and guard plate in a direction parallel to the grid wires. The purpose of the grid was to suppress secondary electrons arising at the back plate behind the grid due to scattered fast molecules. The grid was composed of 0.0008-inch-diameter gold-plated tungsten wires spaced about 0.2 inch apart. It therefore presented a very small solid angle for molecules scattered out of the beam. A potential difference of 360 volts was maintained between the back plate and grid. This prevented secondary electrons arising at the back plate from reaching the collector. The grid-to-collector potential difference was normally 600 volts. The guard plate insured a uniform field over the collection

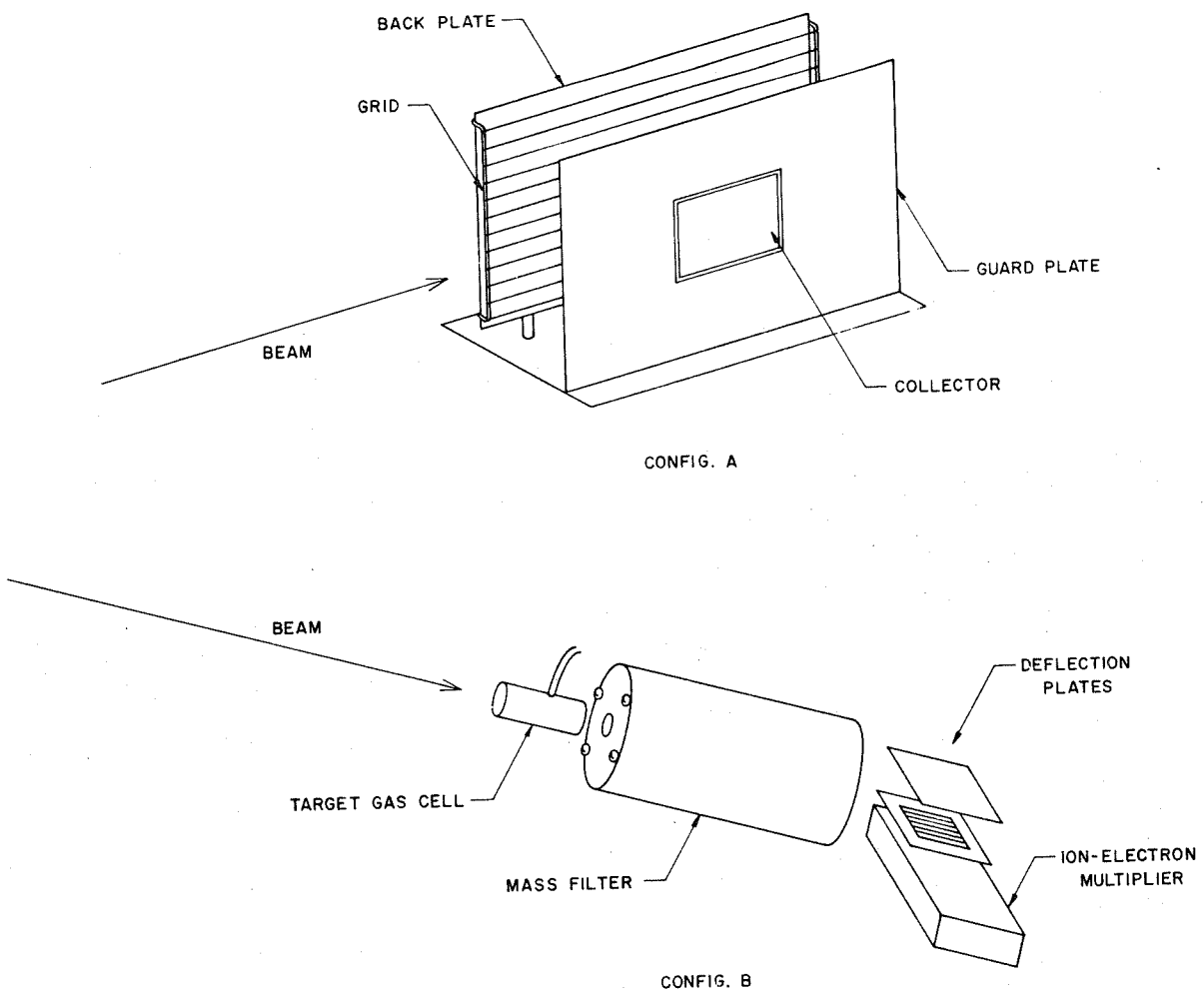


Figure 2 Target Configurations

region and a well-defined collection length. The collector was 10x4 cm, and was spaced 4 cm from the grid. The grid was spaced 1 cm from the back plate. All electrode surfaces were plated with gold.

The electrode assembly was contained in the target chamber, which was evacuated by means of two 6-inch liquid nitrogen-trapped mercury diffusion pumps. The only connection between the beam vacuum system and the target chamber vacuum system was the 3mm exit aperture from the neutralization chamber. This arrangement was used so that the target chamber pressure could be controlled independently of the neutralization chamber pressure. Furthermore, when a target gas different from the neutralizing gas was used, it was essential to keep the target gas as pure as possible. This necessitated continually pumping out the nitrogen, H_2 , or NO which entered the target chamber from the neutralization chamber. During part of the measurements, the electrode assembly was placed inside an "inner target chamber." This will be discussed later.

Target gas was admitted continuously to the target chamber through an aperture pointed so that the gas in the interaction region had diffused off the chamber walls. In this way the pressure gradient in the interaction region was kept small. The pressure calibration was made with a McLeod gauge, an ion gauge, and a capacitance manometer. ⁽⁶⁾

Ion Collection and Current Measurement

The collecting field was maintained between the grid and the collector and guard plate. The distance between was 4 cm. The collector and guard plate were held at ground (chamber) potential, with the grid being made negative. A negative potential of a few hundred volts on the grid sufficed to propel the electrons and negative ions to the collector. Relatively few positive ions then reached the collector, since their energies would have had to be quite high and their directions correct to overcome the field.

The collector plate was connected to a Cary vibrating-reed electrometer driving a strip-chart recorder. It was possible to reliably measure currents smaller than 10^{-16} ampere when charging times of 100 seconds were used.

Consistency Checks and Systematic Corrections

A series of consistency checks which has been developed was applied in each set of cross section measurements. In some cases systematic errors were found and the necessary corrections were obtained in these checks. The techniques have been previously discussed in detail, ^(4, 5) but will be briefly reviewed here. The checks involve collecting field saturation, target pressure saturation, grid efficiency, beam energy-offset in cup, charge transfer slow-ion-current errors, neutralizing gas pressure saturation, and gas mixing effects.

Collecting field saturation was not difficult to achieve in the present work. With a potential of 180 volts on the grid (collector and guard plate grounded) the collected current was within 15% of its value with 900 volts. Essentially no change occurred between 600 and 900 volts. Except during this check, the grid was operated at 600 volts.

The pressure saturation measurements consisted of cross-section measurements taken at several target pressures between 0.5 and 7.5×10^{-4} torr. The usual decrease in cross section was observed with increasing target pressure due to target gas scattering. The normal pressure for measurement was 1.2×10^{-4} torr, and at that pressure the decrease amounted to only a few percent. No large secondary electron effects were observable.

Grid efficiency presented no problem in this work, and was quite adequate. Any secondary electrons arising from the impact of gas-scattered molecules on electrode surfaces gave rise to a current which had the same pressure

dependence as the ionization current. It was therefore not possible to separate this secondary current by varying the pressure. The magnitude of this particular effect was determined in the following manner. If no grid had been present, secondary electrons arising at the back plate due to the impact of gas-scattered molecules would have been accelerated to the collector and would have been indistinguishable from ionization electrons. The grid was added to eliminate this effect. By making the grid sufficiently negative, it was possible to return the secondary electrons to the back plate. However, the grid itself presented a non-zero area to scattered molecules, and secondary electrons arising at the grid could reach the collector. The grid wires constituted about 0.5 percent of the total grid area as seen by scattered molecules. With the grid in operation, the secondary current should therefore have been less than one percent of the current present without the grid. Measurements were made with the grid 0 and 360 volts negative with respect to the back plate (grid-to-collector potential difference = 600 volts). At zero difference in potential, the secondary current should have been about a factor of 100 greater than when the grid was repelling the secondaries arising at the back plate. It was found that with the back-plate-to-grid potential at zero volts, the ionization current less than doubled, indicating that electrons from the grid and back plate could be ignored under usual operating conditions.

A slight beam-energy offset occurs normally in the cup due to the method of monitoring the beam intensity. The i_3 grid does not completely shield the region within it from the cup potential, and the ions are thus normally neutralized in a region of varying potential. This effect may be eliminated if necessary by first measuring β and then making the cup potential zero during the ionization measurement. This does not interfere with the measurement of i_1 , and the beam intensity can therefore still be determined from Eq. (4). This method was used in determining the effective energy offset near threshold for each cross section. It amounted to about 2.0 eV in terms of beam energy, but was easily corrected for.

Since the neutral beam intensity is determined by measuring the current of slow ions produced in the neutralizing gas cell and assuming that each slow ion corresponds to a fast neutral, it is necessary to make an energy analysis of the slow ions in order to consider properly the scattered ions resulting from hard collisions. For previous work involving ground-state beams, this energy analysis was fairly unambiguous due to the large charge transfer cross sections obtained. In the present work on excited beams and charge transfer in NO, the analysis was not as clear, and the possible scattering unaccounted for might have produced as much as a 50% error in the beam intensity. More will be said on this later.

The neutralizing gas pressure was varied by a factor of five to find how much neutral beam scattering and excitation quenching might be occurring due to the neutralizing gas. It was found that at the β 's normally used, the effect was less than 10%.

Gas mixing effects necessitated the largest corrections in the present direct measurements, but the corrections should have been quite reliable. These effects refer to the NO neutralizing gas present in the target gas due to leakage from the neutralization cell into the target chamber, and from target gas present in the neutralization cell due to leakage in the opposite direction. The NO in the target was quite serious because of the large $N_2^* + NO$ cross section at a given beam energy. The target gas in the neutralization cell was serious because of the high charge transfer cross section in the target gas, yielding ground-state beam molecules. These effects could be corrected for by making three separate measurements at each energy: one without target gas but with neutralizing gas, another with target gas but without neutralizing gas, and a third with both target gas and neutralizing gas. By combining these results properly, corrections could be made to the ionization current, which ranged from a few percent to as high as 30%. The final measurements for $N_2^* + CO$

and $N_2^* + N_2$ were made after an apparatus modification, which was intended to decrease the gas mixing corrections. These modifications involved placing the target electrode assembly in an "inner target chamber" inside the diffusion pumped vacuum tank, and differentially pumping the exit aperture from the neutralizing cell. Cross sections (properly corrected for mixing effects) were compared before and after making these modifications and no change was evident even though the magnitudes of the necessary corrections were generally decreased significantly. However, for the particular cases of $N_2^* + CO$ and $N_2^* + N_2$, the corrections under some parameter conditions still ran to 30%. From this consistency, it appears that these corrections are reliable.

DIRECTLY MEASURED RESULTS AND RELIABILITY

Ionization cross section values (more precisely, total cross sections for negative charge production) σ , were obtained from the relationship

$$\sigma = 3.05 \times 10^{-20} (i/PB) \text{ cm}^2, \quad (5)$$

where i is collector current in units of 10^{-16} amp, P is target pressure in units of 10^{-4} torr, and B is the neutral beam equivalent current in units of 10^{-10} amp. The collector length was 10 cm and the temperature was 22°C .

Figures 3 through 10 show directly measured cross sections obtained from Equation 5. Again it must be stressed that because of the ground-state component in the excited molecular beam data, the excited-state results are composite curves of excited-state and ground-state cross sections. The abscissa energy values are kinetic energy in the center-of-mass system minus 11.9 eV for the CO target case, and minus 15.6 eV for N_2 targets. The abscissa values thus equal the excess center-of-mass kinetic energy over the center-of-mass energy thresholds for charge production for a ground-state N_2 molecular beam.

Figures 3 and 7 show the directly measured composite ionization cross sections for $N_2^* + CO$ and $N_2^* + N_2$ respectively. Here, an ion source electron energy of 22 eV was used to produce the N_2^+ ions and they were neutralized in NO. These cross section curves represent lower limits to the excited-state ionization cross sections on an absolute basis. (This is strictly true only where the curves of Figures 3 and 7 are higher than the corresponding ground state curves, Figures 6 and 10. However, other information to be discussed in the next section involving a "no beam" component in measured flux B will justify this statement of lower limit.)

Figures 4 and 8 are composite cross sections for $N_2^* + CO$ and $N_2^* + N_2$ respectively, where the ion source electron energy for N_2^+ formation was 19 eV and again, NO was used as the neutralization gas.

Figures 5 and 9 are composite cross sections for $N_2^* + CO$ and $N_2^* + N_2$ respectively. Here 17.5 eV ion source electrons were used as well as NO neutralization.

Figures 3, 4, and 5 for CO and 7, 8, and 9 for N_2 show the effect of ion source electron energy on the measured results. These curves, along with the results obtained with a pure ground-state beam (Figures 6 and 10), will be useful in the next section in inferring the relative fractions of excited-state and ground-state molecules in the neutral beam, and there from the actual excited-state cross sections.

Figures 6 and 10 are the measured total ionization cross sections for $N_2 + CO$ and $N_2 + N_2$ respectively, where all collision participants were in their ground electronic states. Here the N_2^+ ions were neutralized in H_2 or N_2 . These results are final results and need not be further reduced as the neutral beam composition is known to contain only ground-state N_2 molecules.

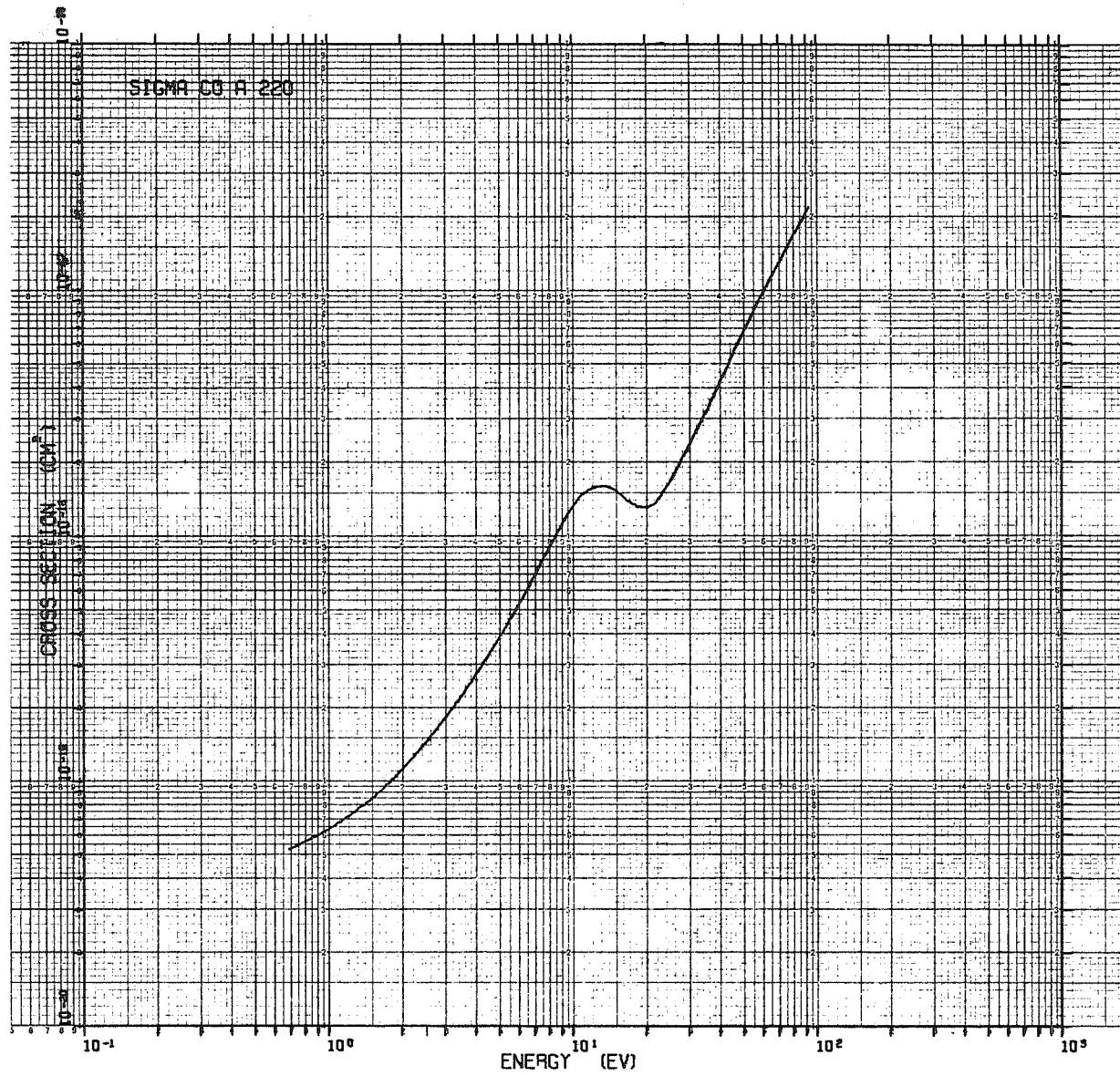


Figure 3 Composite Total Ionization Cross Section for $N_2^* + CO$. Electron Energy 22 eV

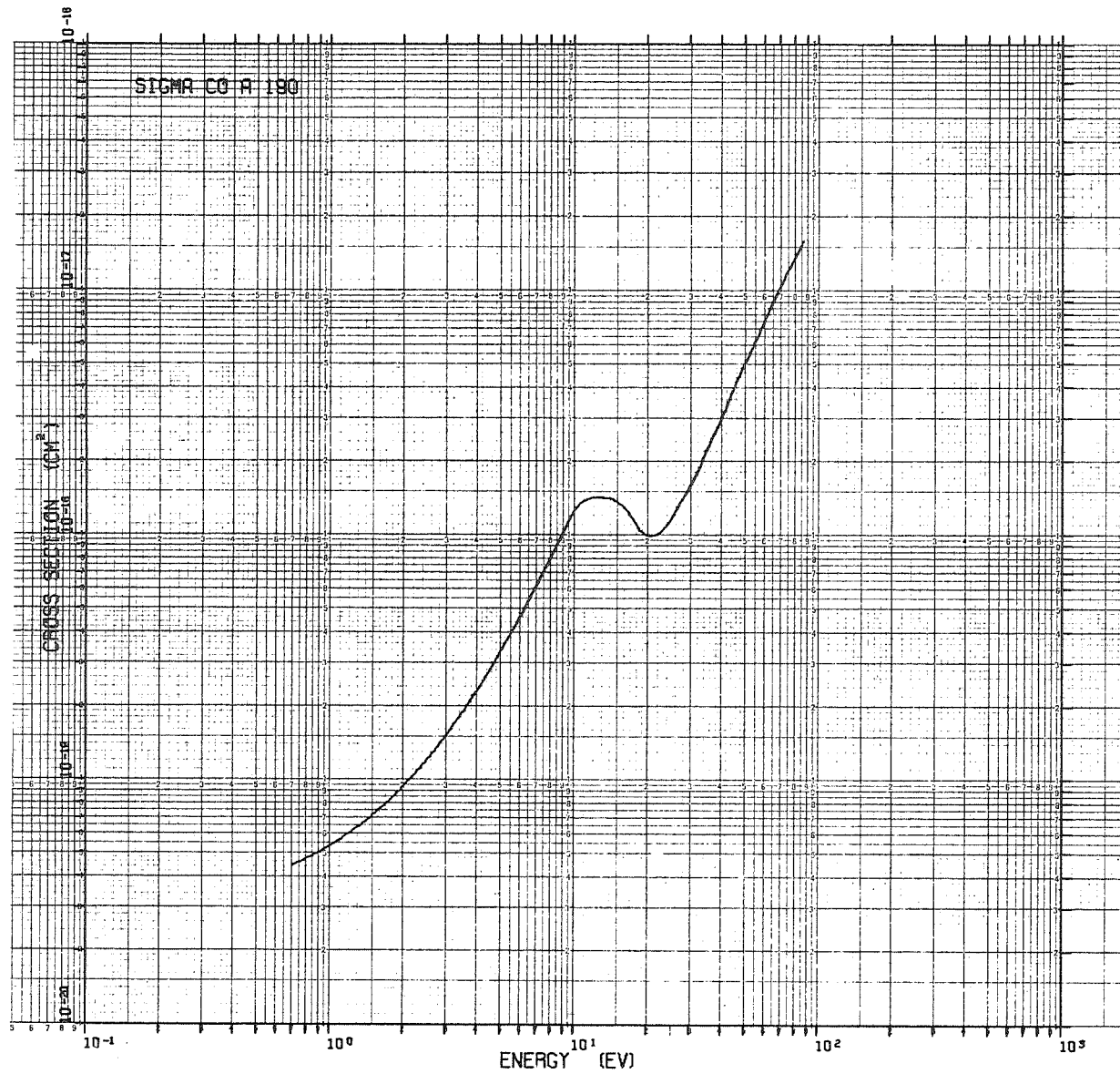


Figure 4 Composite Total Ionization Cross Section for $N_2^* + CO$. Electron Energy 19 eV

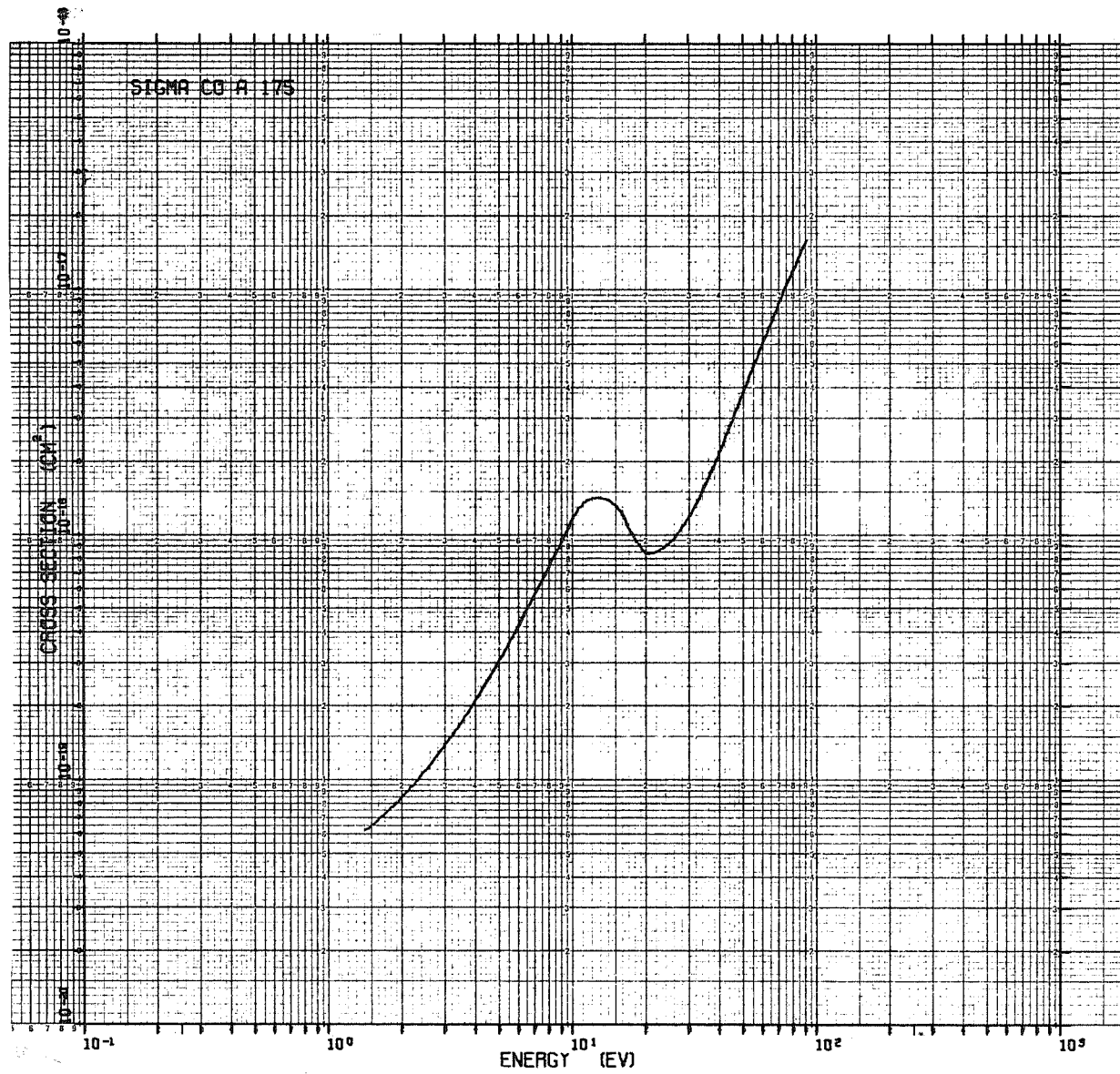


Figure 5 Composite Total Ionization Cross Section for $N_2^* + CO$. Electron Energy 17.5 eV

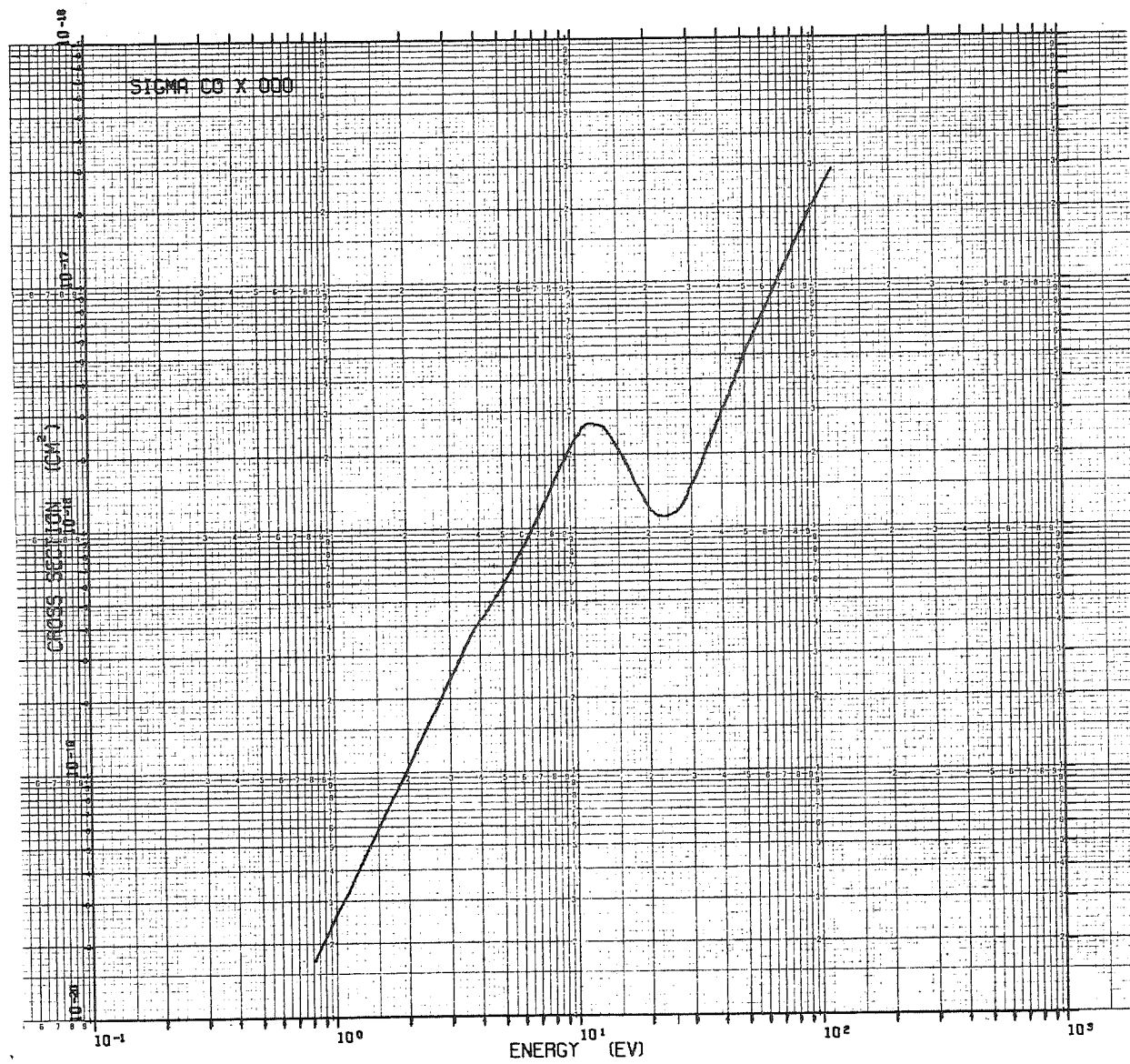


Figure 6 Total Ionization Cross Section for $N_2 + CO$, Ground-State

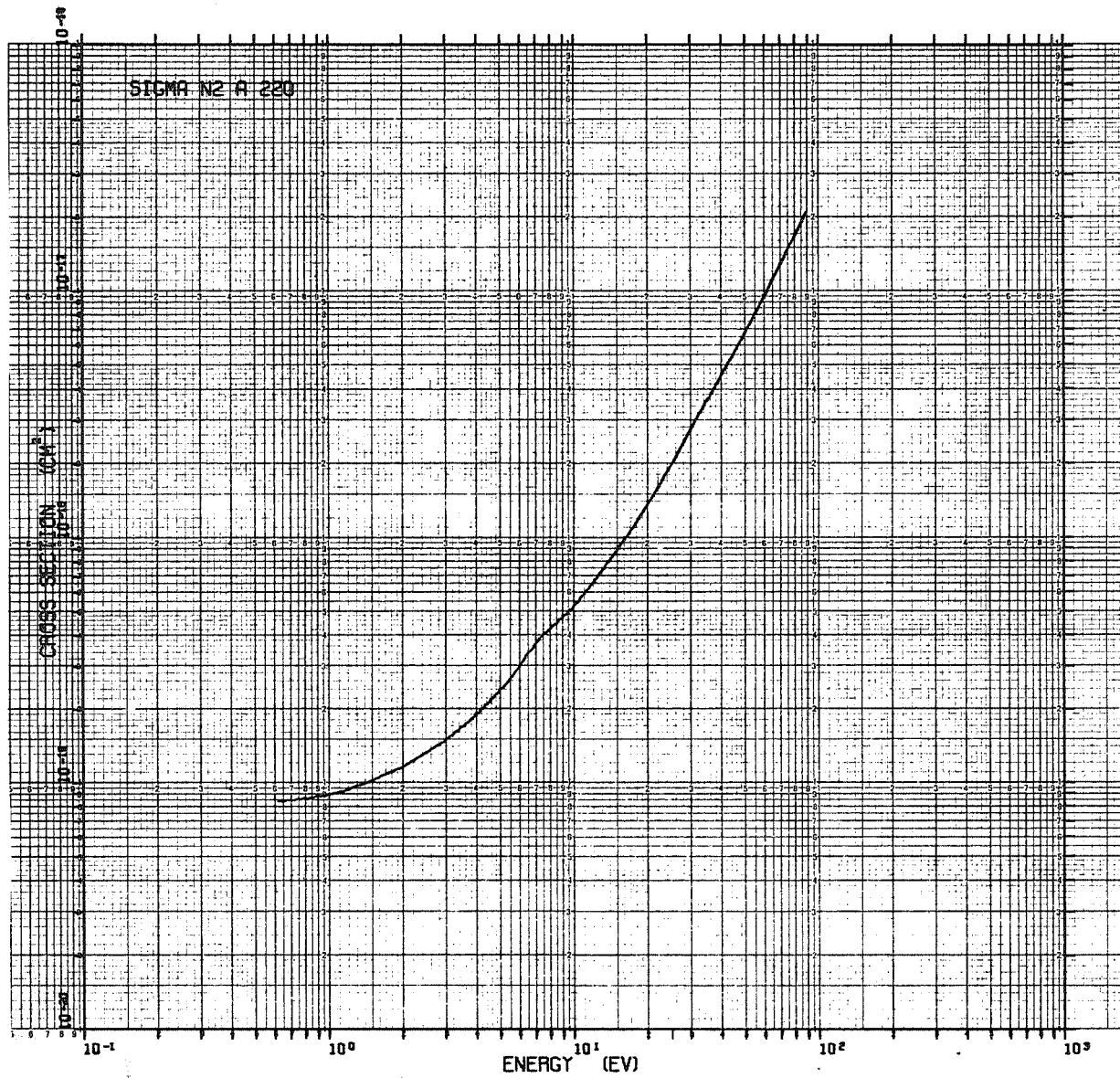


Figure 7 Composite Total Ionization Cross Section for $N_2^* + N_2$. Electron Energy 22 eV

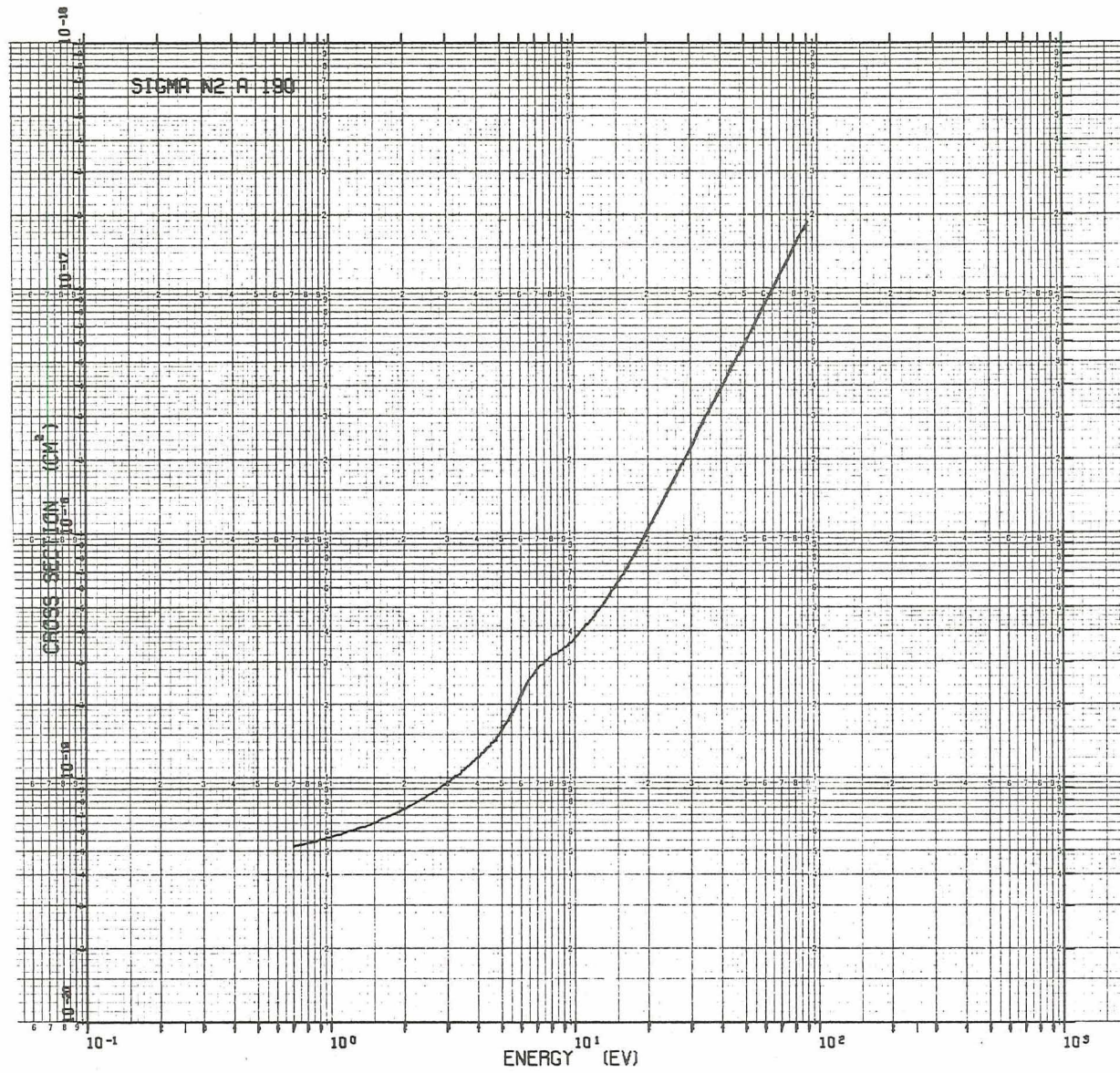


Figure 8 Composite Total Ionization Cross Section for $N_2^* + N_2$. Electron Energy 19 eV

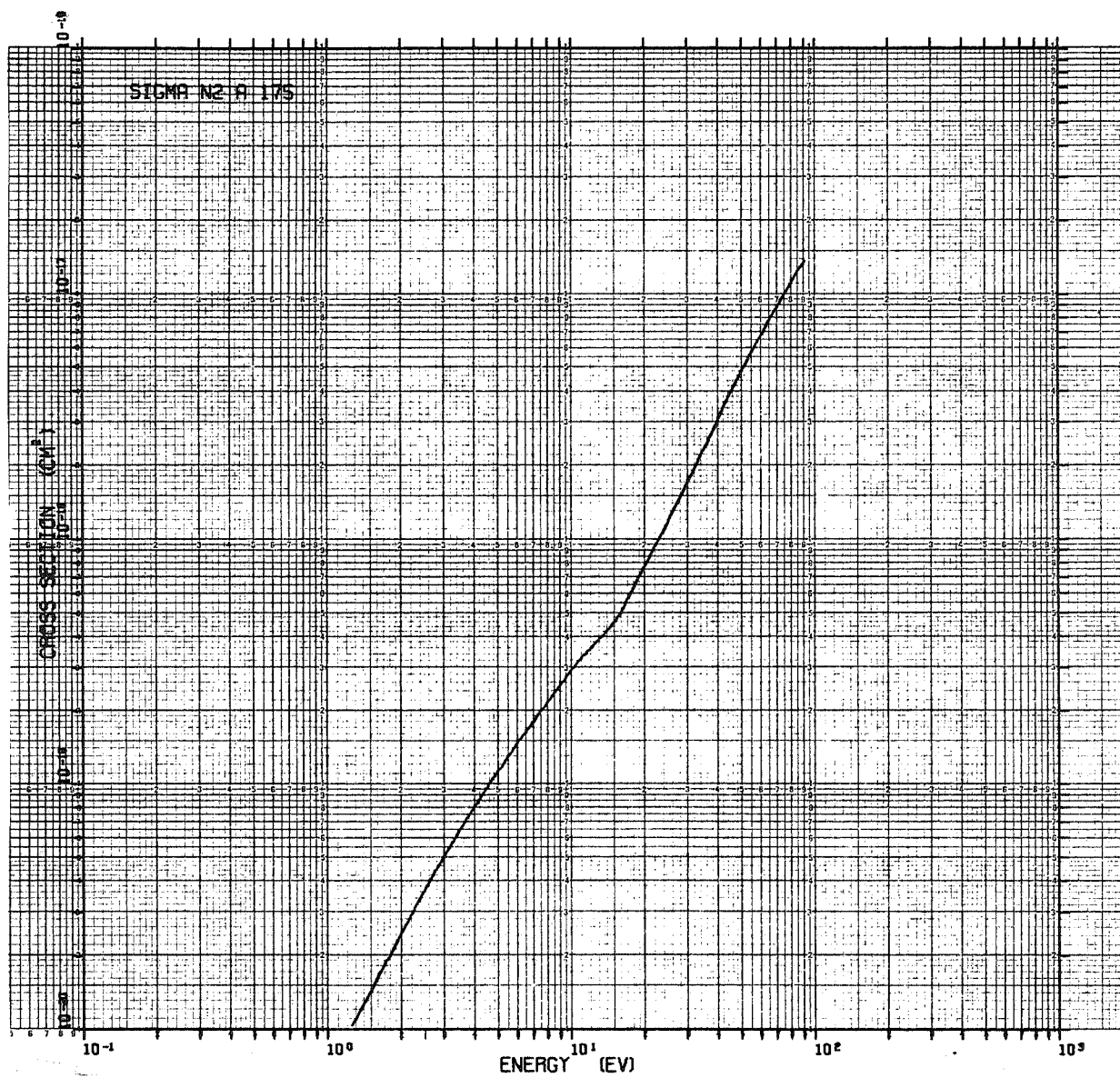


Figure 9 Composite Total Ionization Cross Section for $N_2^* + N_2$. Electron Energy 17.5 eV

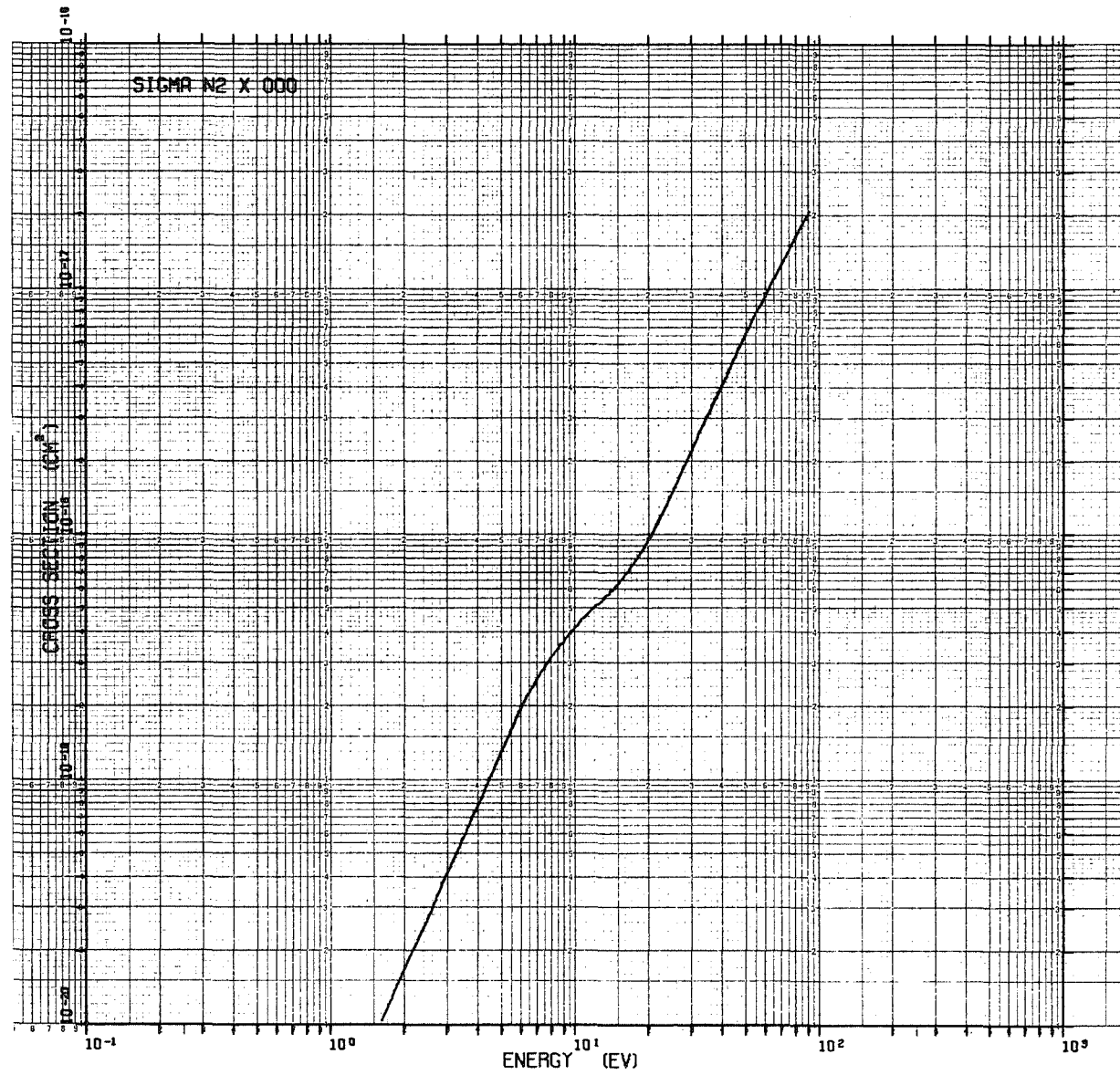


Figure 10 Total Ionization Cross Section for $N_2 + N_2$, Ground-State

With regard to the systematic errors in the determination of the parameters entering Equation 5, the measurements of i and p , with the various corrections discussed earlier, should have been accurate to 10% and 5% respectively. The largest potential systematic error arose from uncertainty in the neutral beam intensity B . Although the total neutral beam intensity is believed known⁽³⁾ to within $\pm 20\%$ for the ground-state neutral beam (used in obtaining Figures 6 and 10), the excited-state beam intensity and composition are more uncertain and are dealt with in the next section. In addition, significant random errors were present in the measurement of i at its lower values, that is, in regions where the cross sections are very small and for low ion source electron energies where flux B is small. Thus, the curves of Figures 6 and 10 (ground-state beam cross sections) should be accurate to $\pm 25\%$ on an absolute basis except near the lower end of the curves where uncertainty increases to $\pm 35\%$. All the curves (Figures 3 through 10) were reproducible on a month-to-month basis to within a few percent, except at the lowest energies where the random errors in i became larger.

BEAM EXCITATION PARAMETER INFERRAL

Excitation Parameters

The key to a method for unfolding the contributions to the composite cross sections from the excited-state beam molecules and those in the ground electronic state was found during a check on possible effects of changing the ion source electron energy. As can be seen by comparing Figures 3, 4, and 5 for CO targets and 7, 8, and 9 for N₂ targets, a sizeable effect is present. Earlier measurements⁽⁸⁾ with targets of Ar, O₂, NO, and a gold surface first pointed up this sensitivity to the ion source electron energy. The ion source electron energy could be varied from 17 eV to 26 eV at given ion beam energies.

Negligible effect on the results was observed for ground-state beam measurements. However, marked effects were noted for N_2^* beam incident on Ar, O_2 , NO, and the gold surface. In each case, a rapid rise (about a factor of two) in the apparent ionization cross section (or secondary emission coefficient) near threshold occurred in changing the electron energy from 17 eV to 19 eV. Furthermore, the shapes of all four cross section vs. electron energy curves near their respective thresholds were very similar from 17 to 20 eV. In this near-threshold region, the measured ground-state ionization cross sections (and the ground-state beam secondary emission coefficient) are small compared to their counterparts wherein excited N_2 molecules participate. The hypothesis made to explain this effect is that the ratio of excited-state to ground-state neutral beam molecules changes with vibrational or electronic state populations in the N_2^+ ion beam, which in turn change with ion source electron energy. Thus, for 17 eV ion source electrons, the excited neutral beam is actually composed largely of ground-state molecules and the fractional excitation of the beam increases with ion source electron energy.

Figures 3 to 10 may be examined in justification of this hypothesis. The progression of "curve shapes" from Figures 3 to 4 to 5 tends toward Figure 6, the pure ground-state results. A similar progression from Figures 7 to 8 to 9 tending to the ground-state beam cross section of Figure 10 exists for the case of N_2 targets. That is, as the ion source electron energy decreases from 22 eV to 17.5 eV, the measured cross section curve shapes approach the ground-state beam cross section. One concludes that, in the case of $N_2^* + N_2$, the actual pure excited-state cross section curve will have very little, if any, structure (at most no more than that shown in Figure 7) as the tendency is for the structure to be reduced by increasing the fraction of the neutral beam molecules which are excited. Similarly, one may conclude that any structure in the true excited-state cross section for $N_2^* + CO$ is smaller than that exhibited by the $N_2 + CO$ pure ground-state reaction result.

(Effects of higher-lying metastable states were also seen in varying the electron energy. Above 22 eV, for example, the $N_2^* + O_2$ ionization cross section rose abruptly. Up to that point, the shape of the cross section vs. electron energy curve was very similar to $N_2^* + Ar$. This is interpreted as being due to higher-lying metastable beam molecules produced by charge transfer of high-lying excited-states of the N_2^+ ion. These metastable neutrals have internal energy sufficient to "Penning ionize" the O_2 . A ratio of about one in 10^4 of such highly-excited molecules in the beam would cause this effect. So long as electron energies below 22 eV were used, the effect caused no problem for O_2 targets. A similar and more serious problem arose for $N_2^* + NO$. Here, with the low 9.3 eV NO ionization threshold, such high-lying metastables appeared to be noticeable down to electron energies of about 19 eV. These interesting but potentially troublesome reactions should not affect the data presented here for CO and N_2 targets.)

It was further found that the composite cross section values for the excited molecular beam increase significantly with increasing electron energy at all beam energies except in the case of $N_2^* + CO$ at a beam energy near the peak in the cross section curve of Figure 6. Here, the composite cross section is essentially independent of electron energy. Since one knows from other targets that the ratio of excited-state to ground-state molecules comprising the excited neutral beam changes with electron energy at this beam energy, this result implies that the cross section for excited-beam molecules and ground-state beam molecules have similar magnitudes at this point. However, the cross section values at that point shown in Figures 3, 4, and 5 are only about one half as large as that given in Figure 6, the ground-state beam case. This feature of the data suggests that the total neutral flux B as determined in the charge transfer cell does not represent the actual neutral flux entering the ionization chamber for the excited molecular beam (NO neutralization).

This uncertainty in the measurement of the total neutral flux B for the excited molecular beam probably results from an ambiguity in the measurement of the slow ion current in the charge transfer cell required for a determination of B. That is, some slow ions captured in the neutralization cell correspond to neutrals which are scattered outside the apertures defining the resultant neutral beam. Hence, a slow ion is collected (contributing to the measured B) which does not contribute to the actual neutral flux. A careful analysis of the charge transfer data suggests that this effect may be present to approximately the degree necessary to explain the observed result. This ambiguity also exists for the ground-state beam case. However, for the ground-state charge transfer reaction (N_2 or H_2 neutralization), the cross section for charge transfer is much larger, and the momentum transfer is proportionately less important.

For purposes of discussion it has been found convenient to classify the excited-state beam according to three components: an excited-state N_2^* (A) component, a ground-state N_2 (X) component, and a "no-beam" component. One can define \emptyset as the excited state component fraction, χ the ground-state component fraction, and ψ the "no-beam" fraction, subject to unit normalization, i. e.,

$$\emptyset + \chi + \psi = 1 \quad . \quad (6)$$

Thus, for example, the actual excited-state neutral flux would be $\emptyset B$ where B is the flux determined in the usual way.

If σ_m represents a typical measured composite cross section, it can be shown to consist of the separate parts,

$$\sigma_m = \emptyset \cdot \sigma_* + \chi \cdot \sigma_x + \psi \cdot 0 \quad , \quad (7)$$

where σ_* is the actual excited-state cross section, σ_x is the measured ground-state cross section, and the zero is due to the fact that the "no-beam" component cannot give rise to any measured signal in the ionization chamber. Here, σ_m would be a cross section such as shown in any of Figures 3, 4, 5, 7, 8, or

9 and σ_x the measured ground-state result as given by Figures 6 or 10. The σ_* is, of course, the true excited-state beam cross section to be determined.

A computer program was written to solve for σ_* in terms of the measured fixed results for σ_x and σ_m (for each of three electron energies) and the parameters \emptyset and ψ which could be varied in a systematic way around reasonable values. For example, it is known that, as discussed earlier, the \emptyset 's must change in the ratios of approximately 1:2:3 as the electron energy ranges from 17.5 to 19 to 22 eV. Similarly, the ψ 's must have values of approximately 0.5 and not change violently with electron energy (from analysis of the charge transfer data). The basic requirement is, of course, that for a particular target gas, the same σ_* curve be generated even though the input σ_m 's, as well as the \emptyset 's and ψ 's, will vary significantly as a function of ion source electron energy. Finally, it is necessary that the same \emptyset 's and ψ 's satisfy the above requirement for both CO and N₂ target gas species.

By this procedure, a reasonable set of parameters approximately satisfying the above conditions and the measured experimental data to within uncertainties has been found. These are shown below.

Electron Energy (eV)	\emptyset	χ	ψ
17.5	0.05	0.475	0.475
19.0	0.09	0.455	0.455
22.0	0.16	0.42	0.42

That these values (or small variations therefrom) represent a "unique fit" to the experimental data and hence generate unique σ_* 's cannot be proven at this point. However, they do meet the requirements imposed upon them by both the input data and the consistency checks stressed in the method.

Inferred Excited-State Cross Sections

The cross sections for ionization inferred from the above analysis for collisions between excited nitrogen molecules and CO and N₂ targets are shown in Figures 11 and 12 respectively. These curves (particularly that for the CO target) have been "smoothed" slightly from the actual computer outputs which are very sensitive to small experimental fluctuations in the measured data. The beam composition parameters (i. e., the θ , χ , and ψ) listed in the previous section were used here.

Consider first the result shown in Figure 12 for N₂ targets. It was mentioned earlier that the trend in the composite cross section shape as the beam excitation fraction increases suggested that the pure excited-state beam result should have little or no structure. It can be seen in Figure 12 that the inferred excited-state cross section curve verifies this earlier suggestion. Small variations in the beam composition parameters do not appear at this time to grossly change the basically smooth cross section curve shape.

In contrast, the inferred excited-state cross section curve for CO targets shown in Figure 11 does exhibit a small structure in the 12 eV excess energy region. Unfortunately, however, in this case the presence of structure is very sensitive to the beam composition as the ground-state beam cross section exhibits a large structure peak here. Hence only the general trend of the curve should be taken seriously at this time. In any case, no structure comparable to that displayed in Figure 6 for the ground-state beam reaction is evident. Again, this result verifies the earlier suggestion and, furthermore, indicates that the specific reaction processes which occur using the excited beam are different from those dominating the ground-state beam reactions.

In an attempt to more closely evaluate the beam composition parameters θ , χ , and ψ and thereby more accurately determine the excited-state beam

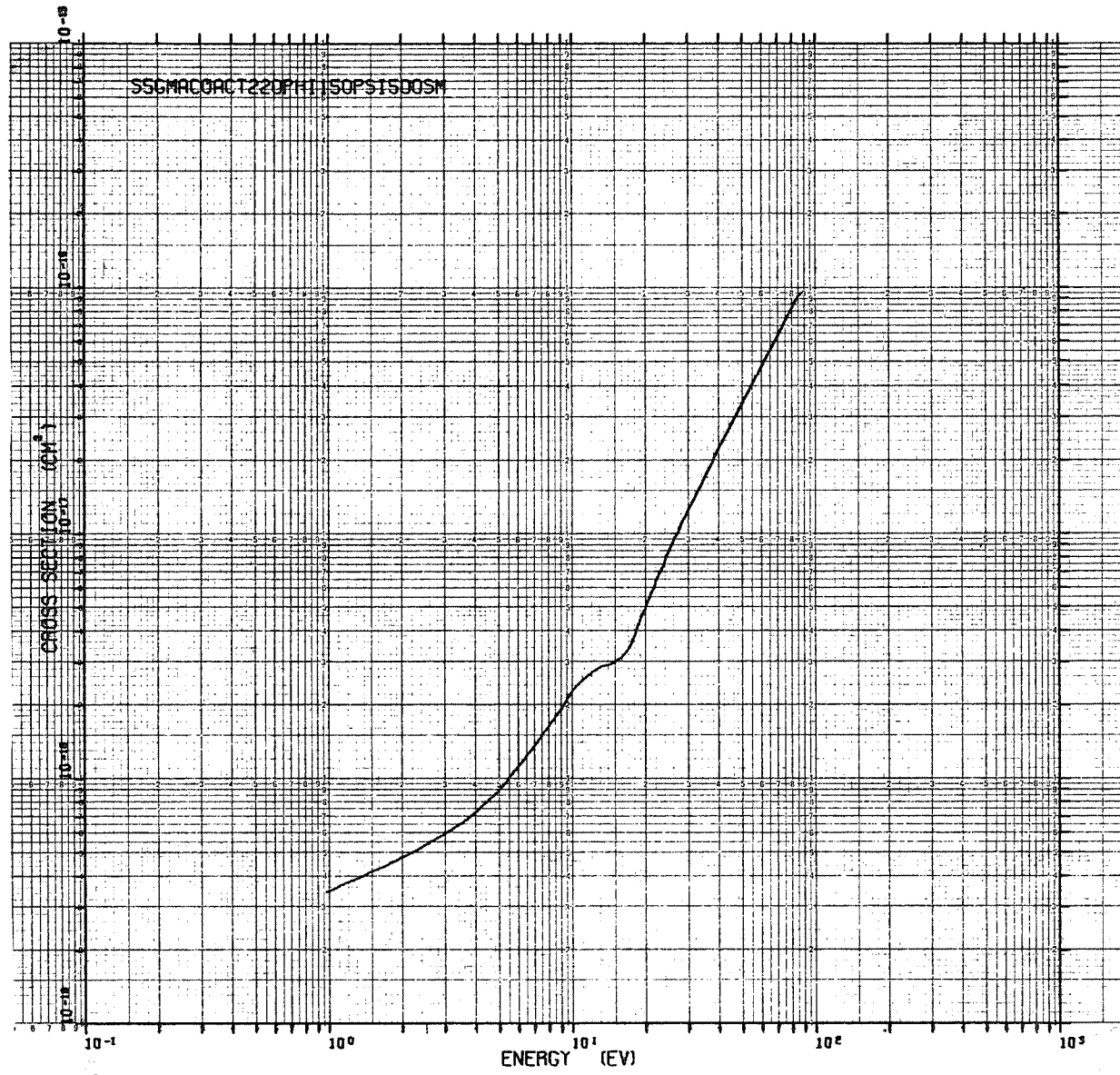


Figure 11 Inferred Total Ionization Cross Section for $N_2^* + CO$. Excited-State

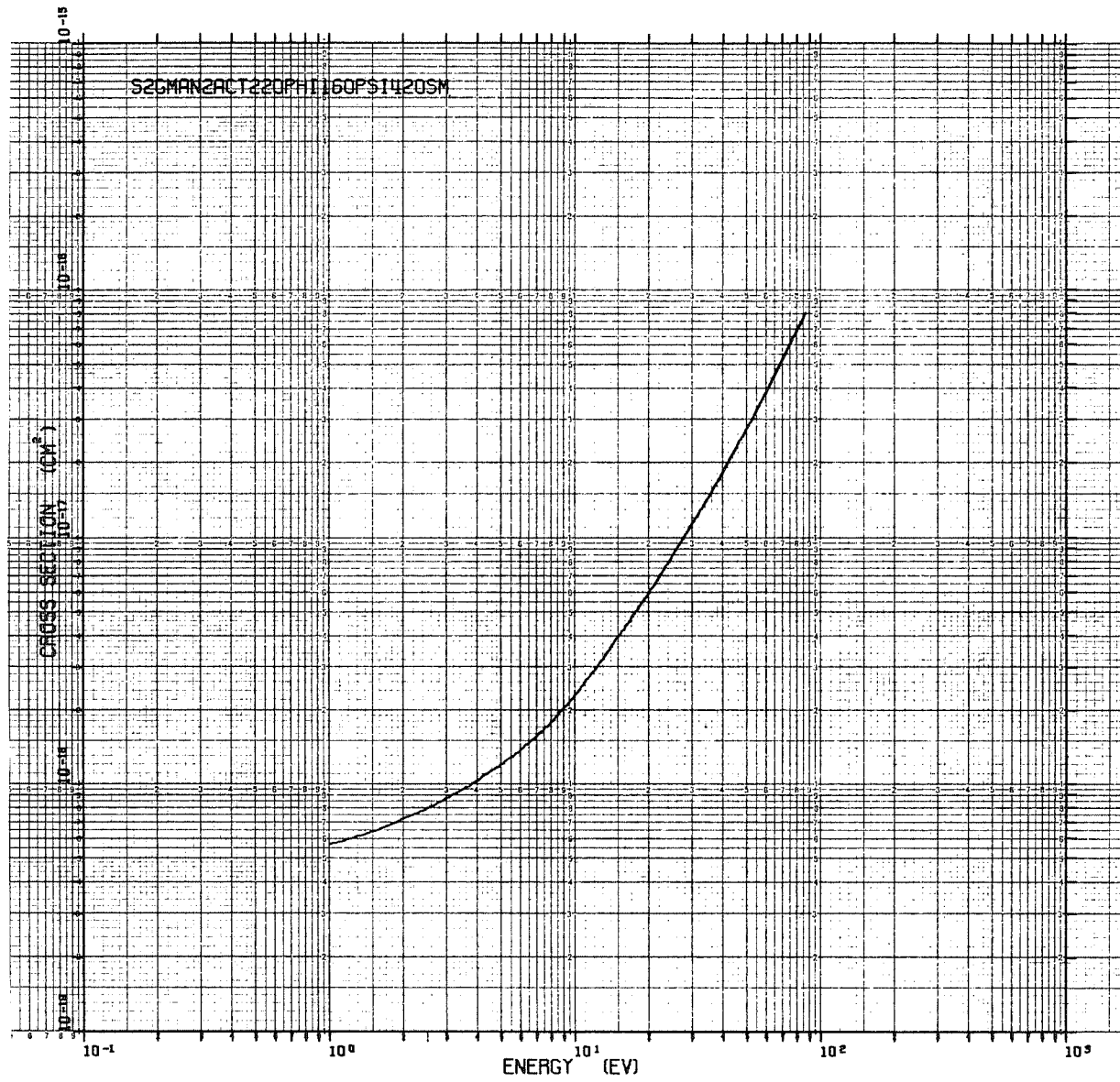


Figure 12 Inferred Total Ionization Cross Section for $\text{N}_2^* + \text{N}_2$. Excited-State

ionization cross sections, a second computer program has been prepared. This program, in effect, performs operations in reverse to those described above. For its input, it requires the experimentally determined ground-state beam cross section σ_x and a previously inferred, but slightly "smoothed" excited-state beam cross section σ_* . After including the appropriate beam composition parameters, it generates composite cross section curves which can be compared directly to the experimentally measured composite cross sections at the three different electron energies used here. It is felt that this procedure should be less sensitive to small fluctuations in the experimental data.

Only very preliminary results from the new program output are available at this time. Using the ground-state cross sections of Figures 6 and 10, the inferred excited-state data of Figures 11 and 12, and the beam composition fractions suggested earlier, composite cross section curves were generated and compared with their experimentally measured counterparts as shown in Figures 3, 4, 5, 7, 8, and 9. For CO targets, the agreement was quite good. On the other hand, the comparison for N_2 targets pointed out a possible effect not yet investigated in detail. In this case, the computer-generated and experimentally-measured composite cross sections agreed well from 100 eV down to about 15 eV excess energy. Below this energy, however, the computer generated result fell below the measured curve. This divergence increased as the excess energy decreased, the difference being about 40% at the lowest energies. In all probability, the cause of this effect is a functional dependence of the beam composition parameters on the collision energy. That this effect was much smaller for CO targets can be readily understood. In the CO case, the excited-state and ground-state cross section values are not grossly different and hence small changes ($\sim 25\%$) in the already small excited-state beam fraction ϕ will not appreciably modify the composite curve. For N_2 , on the other hand, the excited-state cross section dominates the composite curves

at the lower energies and hence small changes in θ as a function of collision energy are directly reflected in the data. The cause of this effect will be discussed later.

MASS SPECTROMETER MEASUREMENTS

A mass spectrometer was incorporated into the neutral-neutral scattering apparatus for purposes of making an identification of the ionic collision products. For these studies, a small target gas cell was placed in front of the entrance aperture of a quadrupole mass filter and the incident molecular beam was directed through the cell along the mass filter axis (Figure 2, target configuration B). Product ions ejected within a roughly 6° half-angle cone passed into the mass filter wherein positive ions were analyzed as to mass. No pre-acceleration into the filter was employed. Ions of the appropriate mass, upon traversing the filter were accelerated to the face of an ion-electron multiplier. Pulse counting techniques were employed and counting rates down to about one per second were used. The pulse counting procedure was found to be more satisfactory than the earlier method of measuring multiplier DC currents.⁽⁷⁾

Mass spectrometer measurements were made for both excited and ground-state nitrogen molecular beams on CO and O₂ targets.

Mass spectrometer results for ground-state nitrogen molecules on CO targets have been reported earlier.⁽⁷⁾ The interesting process



was found to be the dominant charge producing reaction at the lower energies in collisions between ground-state N₂ and CO molecules and largely accounts for the well-defined peak structure exhibited by the curve of Figure 6. Some

mass 28 ions (N_2^+ or CO^+) were also observed but in amounts significantly less than the mass 30 ion (NO^+). Above about 30 eV excess energy in the center-of-mass system, dissociative ionization leading to the atomic ions C^+ , N^+ , and O^+ was observed, and became more prevalent as collision energy increased.

The present measurements made with the improved pulse counting techniques largely substantiate these older results. The improved sensitivities now available, however, allowed the present studies to be made at lower target cell pressures. At the lower pressures, more mass 28 ions were observed than before. As the CO target pressure was increased the ratio of mass 28 to mass 30 ions decreased indicating that some of the mass 28 ions were CO^+ (as opposed to N_2^+) and that those CO^+ ions were resonantly charge transferring with the target CO molecules and, hence, not reaching the final ion collector. Subsequent studies were made at lower pressures where such secondary effects could be ignored. The new sensitivity also allowed detection of small amounts of CN^+ as a collision product. Thus, all possible product ion masses were observed. Once again, however, the dominant low energy process was found to be that of Eq. (8).

Some data on the mass analyzed products of the ground-state $N_2 + O_2$ collisional system were also previously reported.⁽⁹⁾ Here again it was found that an ion exchange reaction similar to Eq. 8 gave the dominant charged collision product up to about 40 eV excess energy. This reaction,



was identified by observation of the NO^+ product. In contrast to reaction (8) above (wherein both NO^+ and CN^- were observed with the mass filter), the NO^- ion could not be here detected. It is likely, however, that if the NO^- ion were produced as an initial product, it would readily lose its barely-bound

electron in collisions with the background gas. Again, at the higher energies, the presence of N^+ and O^+ suggests the importance of the dissociative ionization processes in this energy range.

The new results for ground-state $N_2 + O_2$ collisions once again substantiate this older data. Also detectable now are mass 28(N_2^+) ions and mass 32(O_2^+) ions at the lower energies even though the relative amounts of those ions are much smaller than the mass 30(NO^+) species.

While the new mass spectrometric results using ground-state nitrogen molecular beams on CO and O_2 targets proved interesting and identified previously undetected reaction channels at lower energies, the results obtained using the excited molecular beam were less quantitative. This is largely due to the difficulty associated with interpretation of those results because of the small numbers of excited-state molecules present in the beam and hence the domination of the results by the ground-state collision processes. In spite of those limitations, important information was obtained.

For both CO and O_2 targets, the relative efficiencies for producing N_2^+ ions in the collision processes are significantly enhanced by the use of the excited molecular beam as compared to the ground-state beam. This suggests that the simple direct ionization process is relatively much more important if the incident neutral molecules are in their $A^3\Sigma_u^+$ excited state. Whether or not such ion exchange reactions as described by Eqs. (8) and (9) occur with excited-state molecules cannot be determined at this time. If they do, however, their relative importance must be significantly less than in the corresponding ground-state beam results.

One other by-product of the mass spectrometric work should be discussed. This is concerned with the ratio of the height of the mass 30(NO^+) peak to the

spectrometer background level for both excited and ground-state beams on CO targets. The NO^+ ion peak results from the production of NO^+ ions in the target gas cell. The spectrometer background level, however, arises from the neutral beam projectiles traversing the mass filter and producing ionization in the residual target gas in the vicinity of the final ion collector and hence must be proportional to the total ionization cross section (after correcting for non-target gas backgrounds). At that energy where the excited and ground-state cross sections are nearly equal, the ratio of NO^+ peak height to total ionization background decreased by 12% when the excited-state beam was substituted for the ground-state beam. Thus one can conclude that the excited-state beam contains at least 12% fewer ground-state molecules than the ground-state beam and hence, that the true excited-beam must be composed of a minimum of 12% excited molecules at 22 eV electron energy. Including the "no-beam" component discussed earlier, one can thus conclude that the minimum value of ϕ for 22 eV electrons is of order 0.06. The "best fit" value of 0.16 selected earlier is consistent with this minimum value requirement.

DISCUSSION

The most striking feature of the present results is the significant enhancement of the total ionization cross section for neutral N_2 molecules on CO and N_2 targets when a neutral beam containing $\text{A}^3\Sigma_u^+$ molecules is substituted for the ground-state nitrogen molecular beam. This conclusion is independent of how the present data are reduced and can be seen by consideration of the measured results only. This result substantiates a similar conclusion reached for studies using Ar, O_2 , and NO as target collision partners and discussed previously. ^(2, 8) In addition, data obtained by mass analysis of product ions scattered in the forward direction show that the relative importance of simple direct ionization of the N_2 neutral from its $\text{A}^3\Sigma_u^+$ level is significantly greater than the corresponding process when ground-state $\text{X}^1\Sigma_g^+$ molecules are used.

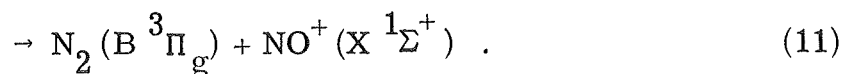
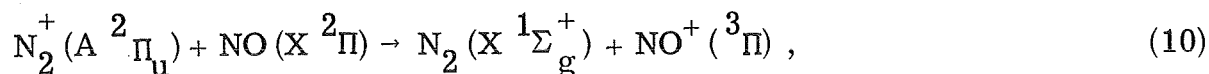
The actual ionization cross sections for collisions between excited-state nitrogen molecules and CO and N_2 targets have been inferred in this report by making an assessment of the fraction of excited nitrogen molecules in the excited-beam (i. e., that resulting from N_2^+ neutralization by charge transfer in NO). This was accomplished by subjecting a computer program containing variable parameters to experimentally determined boundary conditions on these parameters and then searching for values giving a "best fit" to the experimental results. These parameters identify the fraction of excited molecules (θ), the fraction of ground-state molecules (χ), and the "no beam" fraction (ψ) present in the apparent neutral beam of flux B. The accuracy of these inferred cross sections depends, of course, on the accuracy with which these beam composition parameters were evaluated.

For the inferred cross sections presented in Figures 11 and 12, it was assumed that the beam composition parameters were independent of collision energy. This assumption can hardly be expected to rigidly hold as the details of the charge transfer process setting the parameters will almost certainly depend upon ion kinetic energy (which, of course, determines the neutral product energy). The new computer program described earlier has already demonstrated that this assumption is invalid. The parameters listed in this report are probably most accurate in the 10 to 15 eV excess energy region. It appears at this time that the parameter θ for 22 eV electrons should be closer to about 0.12 at the lowest energies considered here and perhaps reach 0.20 or higher in the vicinity of 100 eV excess energy. This variation would imply that the true excited-state cross sections presented here are about 25% low at the lowest energy points and approximately 20% high near 100 eV. A more accurate evaluation of this effect must await additional study.

This report will now be concluded with a brief discussion of the charge transfer process for $N_2^+ + NO$ which must be understood in more detail for more accurate assessment of the beam composition parameters.

A crude analysis of the process of electron impact ionization in the ion source and an approximate computation of flight times of extracted N_2^+ ions from the source to the charge transfer cell allow a rough estimate to be made of the composition of the N_2^+ ion beam at its point of neutralization. These considerations suggest that as the electron energy is varied from about 17 eV to 22 eV, the fraction of the ion beam in the $v=0$ vibrational level of ground electronic state $N_2^+(X)$ decreases from about 0.6 to 0.4. In order for this ion to charge transfer efficiently, two conditions must prevail: an energy resonance (or near resonance) to a final fast neutral and slow ion must be available, and the Frank-Condon factors for the transitions of initial ion to final neutral and initial neutral to final ion must be sizeable. These conditions are not met closely if the initial ion is in its $N_2^+(X, v=0)$ level. Hence, the charge transfer efficiency of this level should be small and probably occurs only with some momentum transfer during the collision. Some of the "no-beam" components may result from this process.

Thus, it appears that at least part of the real neutral flux arises from $N_2^+(X)$ ions in vibrationally excited states. The $v=1, 2, 3,$ and 4 levels of the $N_2^+(X)$ ion are all present in the ion beam and the sum of their populations increases from about 0.4 to 0.5 of the total ion beam as the electron energy increases from 17 to 22 eV. A third component in the beam appears to consist of $N_2^+(A)$ ions which, by virtue of their long lifetimes ($\sim 12\mu\text{sec}$), have not yet all decayed to $N_2^+(X)$ ions upon arrival at the neutralization cell. This fraction of the beam varies from approximately 0.01 at 17 eV to about 0.1 at 22 eV. $N_2^+(A)$ ions appear to be good candidates for charge transfer in NO by either of the reactions:



Reaction (10) leaves the N_2 in the ground electronic state and reaction (11) leaves the neutral N_2 in its $N_2(B)$ level which in turn rapidly decays to the $N_2(A)$ state. Here again, as with $N_2^+(X)$ ions, competing reactions share the total neutralization probability and give rise to both $N_2(X)$ and $N_2(A)$ neutral beam products. That $N_2^+(A)$ ions do participate in generation of the $N_2(A)$ excited beam has been demonstrated by measurements in which the ion flight time (and hence, the time allowed for decay of the $N_2^+(A)$ level) from the ion source to the neutralization cell was varied. Small changes in the fraction of excited molecules present in the NO neutralized beam as a function of ion flight time were observed. Preliminary studies suggest that this contribution, while clearly present, may not be sufficient to account for all the excited molecules in the beam. It is interesting to note, however, that reaction (11) provides a channel for excited neutral beam production which varies with electron energy in a way consistent with the experimental result. In addition, this process can at least partially explain the variation of the parameter θ with collision energy. The flight time for ion transit from their source to their point of neutralization depends on the beam kinetic energy. At the lower kinetic energies, the $N_2^+(A)$ ion beam component is small since the reduced ion velocity and hence, the increased flight time allows most of these ions to decay to the $N_2^+(X)$ ground-state level. However, at higher collision energies where these transit times are shorter, more of the $N_2^+(A)$ ions reach the neutralization cell thus increasing the contribution made by reaction (11).

It thus appears that the process of generation of an $N_2(A \ ^3\Sigma_u^+)$ molecular nitrogen beam by neutralization of N_2^+ ions in NO is very complex. However, while the discussion immediately above must be considered only in a qualitative sense, it appears that progress is being made toward understanding of the complicated phenomena occurring.

REFERENCES

1. C. F. Hansen, Proceedings of the Sixth International Symposium on Rarified Gas Dynamics, M. I. T. 1968, Academic Press, 1969.
2. N. G. Utterback and B. Van Zyl, Phys. Rev. Letters 20, 1021 (1968).
3. N. G. Utterback and G. H. Miller, Rev. Sci. Instr. 32, 1102 (1961).
4. N. G. Utterback and G. H. Miller, Phys. Rev. 124, 1477 (1961).
5. N. G. Utterback, Phys. Rev. 129, 219 (1963).
6. N. G. Utterback and T. Griffith, Jr., Rev. Sci. Instr. 37, 866 (1966).
7. N. G. Utterback, J. Chem. Phys. 44, 2540 (1966).
8. N. G. Utterback and B. Van Zyl, AC-DRL Tech. Report No. TR68-65 (1968).
9. N. G. Utterback, Proceedings of the Fifth International Conference on the Physics of Electronic and Atomic Collisions, Leningrad, Publishing House Nauka, 216 (1967).